Journal of
Chemical and Process Engineering

JScholar
Fostering Scholarly Communication

Research Open Access

A Polymer-Assisted Hydrothermal Approach to Titanium Dioxide Thin Films

Qianglu Lin, Yuling Li, Brian Patterson, Hongmei Luo*

Department of Chemical and Materials Engineering, New Mexico State University, Las Cruces, NM 88003

***Corresponding author:** Hongmei Luo, Department of Chemical and Materials Engineering, New Mexico State University, Las Cruces, NM 88003; E-mail: hluo@nmsu.edu

Received Date: September 26, 2014 **Accepted Date:** November 11, 2014 **Published Date:** November 13, 2014

Citation: Hongmei Luo, et al. (2014) A Polymer-Assisted Hydrothermal Approach to Titanium Dioxide Thin Films. J Chem Proc Eng 1: 1-6.

Abstract

Epitaxial anatase TiO_2 thin films on $LaAlO_3$(001) substrates are prepared by a novel polymer-assisted hydrothermal method. The titanium ions binding with ethylenediaminetetraacetic acid (EDTA) and polyethyleneimine (PEI) result in a homogeneous clear stable precursor solution followed by hydrothermal for thin film deposition. High resolution transmission electron microscopy analysis shows that the film has two layers with one densely deposits onto the substrate while the other contains nanopillars stacking onto the former layer. The phase, epitaxy, and film thickness can be controlled by metal precursor concentrations, pH, temperature, and reaction time. In addition, TiO_2 and SiO_2-embedded in TiO_2 composite films directly grown on Ni foam are investigated as anodes for lithium-ion battery application.

Introduction

Due to its numerous applications in a wide variety of fields, there has been intensive research on the growth of titanium dioxide (TiO_2) [1-21]. Several techniques have been applied to grow thin films, such as sputtering [12,13], pulsed-laser deposition [14,15], molecular beam epitaxy [16,17], electron-beam evaporation [18], and chemical vapor deposition [19,20]. However, high vacuum and high temperature of these processes have limited the potential application of films. Polymer-assisted deposition [21-23], sol-gel, hydrothermal and other solution approaches [7,24,25] have become more attractive alternatives for thin film deposition because of their low cost, large area, and low temperature fabrication [22].

Hydrothermal favors the formation of thicker thin films than other solution spin- coating methods. Liquid phase hydrothermal deposition has been applied to prepare epitaxial oxide thin film [24-27]. However, the precursor solution for thin film growth by hydrothermal was not clear solution and the films were formed by stacking oxide powders, which created voids inside the films. A variety of high quality epitaxial metal oxides and oxide nanocomposite thin films without voids can be grown by polymer- assisted deposition [21-23,28], where the metal-polymer solutions are clear and stable solutions, however, the thickness of resulted thin films is usually less than 100 nm even by controlling the solution concentration and multiple spin-coats. In this paper, we combine polymer-assisted deposition with hydrothermal method, named polymer-assisted hydrothermal, in order to achieve thicker films of metal oxides and oxide nanocomposites. We report dense epitaxial TiO_2 thin films and epitaxial SiO_2-TiO_2 composites grown on single crystal $LaAlO_3$ (LAO) (001) substrates. This method provides a safe and environmental friendly path for thin film deposition and avoids the use of fluoride ligand in the liquid phase deposition.

Since TiO_2 nanostructures have been widely studied as anode material for lithium ion batteries [29-38], we further use nickel foam instead of single crystal LAO substrate in the polymer-assisted hydrothermal synthesis to prepare TiO_2 and SiO_2-TiO_2 composites for the anodes. Since nickel foam is a polycrystalline substrate, not single crystal substrate, therefore the films on nickel foam are polycrystalline films, not epitaxial films. This one-step binder-and-conductive carbon-free process makes the contact between TiO_2 and current collector (nickel foam) more stable and is expected to improve the battery performance.

Experimental

Synthesis of anatase TiO_2 thin film on LAO substrate

The titanium solution (0.5mL titanium tetrachloride was added dropwise into 3mL of 30 wt% hydrogen peroxide) was added to a solution containing 2g of 50 wt% polyethylenimine (PEI), 1g of ethylenediaminetetraacetic acid (EDTA), and 40mL of deionized (DI) water to form a bright orange solution. During this process, the pH of the solution was maintained at 7.5. The as-prepared titanium precursor solution was transferred into a Teflon-lined autoclave and the final pH of the solution was adjusted by ammonium hydroxide or hydrogen chloride.

The LAO substrate was washed by a mixture of 50% of concentrated hydrogen chloride and 50% of hydrogen peroxide with sonication for 10min to remove contaminants on the substrate. Then the substrate was placed on the Teflon holder with its polished side facing down in a Teflon-lined stainless steel autoclave with 12mL precursor solution. The reaction temperature, time, pH, concentrations were examined to explore the optimum condition for epitaxial thin film deposition. Detailed reaction conditions are listed in Table 1. After the hydrothermal process, the films were washed with deionized water and dried at room temperature.

Sample	Time (hours)	Temperature (°C)	pH	Concentration (mM)
A	6	200	7	20
B	9	200	7	20
C	12	200	7	20
D	24	200	7	20
E	24	150	7	20
F	24	200	7	20
G	24	200	4	20
H	24	200	7	20
I	24	200	10	20
J	24	200	7	20
K	24	200	7	200

Table 1: Reaction conditions for TiO_2/$LaAlO_3$ thin film deposition.

Synthesis of SiO_2-embedded in TiO_2 thin film on LAO substrate

The precursor solution was prepared by mixing different concentration of silica (The commercial Ludox silica nanoparticles with sizes around 10 nm bind to PEI, the concentration of silica is 460mM) with titanium solution. LAO substrates were placed into the Teflon-lined stainless steel autoclave as mentioned above for thin film deposition. For a complete deposition, the reaction conditions were controlled at 200°C for 24 h.

Characterization of thin films on LAO

The structures of the products were characterized by X-ray diffraction (XRD) with a Rigaku Miniflex II X-ray powder diffractometer with CuKα (λ=0.15406nm) radiation. A Hitachi High Technologies H-7650 transmission electron microscope (TEM) operated at 80kV, a Hitachi Model S-3400N Type II scanning electron microscope (SEM) and an atomic force microscope (AFM) were used to characterize the morphology and microstructure of samples. The composition of SiO_2-embedded in TiO_2 thin film was analyzed by energy dispersive X- ray spectroscopy (EDS).

Preparation and electrochemical performance of lithium-ion batteries

The nickel foam was used as the substrate to grow TiO_2 and SiO_2-TiO_2 films. The nickel foam was immersed in the titanium precursor solution with or without SiO_2 nanoparticles into an autoclave and treated at 200°C for 24h. To prepare the lithium ion battery, coin cells were assembled in an argon-filled dry glove box. Metal lithium was used as a counter electrode, whereas the electrolyte contained 1M $LiPF_6$ in a mixture of ethylene carbonate (EC) / dimethyl carbonate (DMC) with 1:1 volume ratio. Galvanostatic charge/discharge cycling performance were evaluated on an LAND Battery Tester CT2001A at a room temperature in a potential range of 0.005-3.00V (versus Li+ / Li) at different current densities.

Result and Discussion

Figure 1(a) shows the XRD θ-2θ scan of TiO_2 on LAO substrate by hydrothermal reaction. The preferential (004) diffraction peak from anatase TiO_2 indicates the thin film deposits on (001) LAO single crystal substrate with highly c-axis orientation. Figure 1 (b) shows the in-plane ϕ-scan between TiO_2 (101) and LAO (101), in which four peaks with 90° separation identifies the epitaxial nature of the film. The epitaxial relationship can be described as

(001)TiO_2||(001)LAO and [101]TiO_2||[101]LAO.

Cross-section TEM images of TiO_2 thin film deposited on (001) LAO substrate at 200°C for 12 hours are shown in Figure 2. The film thickness is around 700nm. Two layers of TiO_2 nanostructure are observed with one densely deposits onto the LAO substrate while the other contains nanopillars stack-

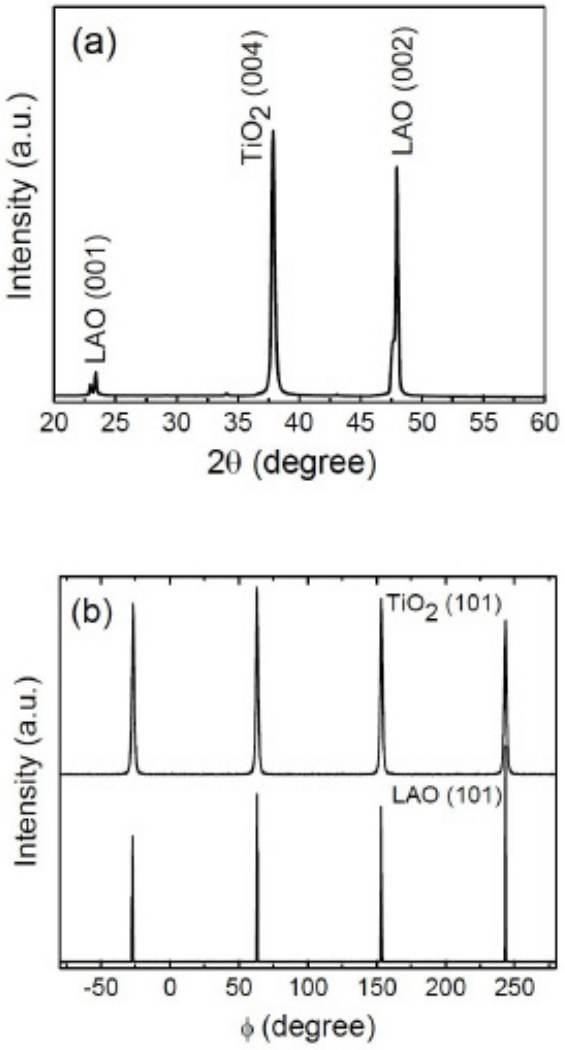

Figure 1: XRD patterns of TiO_2 thin film on LAO substrate. (a) θ-2θ scan; (b) ϕ-scans of TiO_2 (101) and LAO (101).

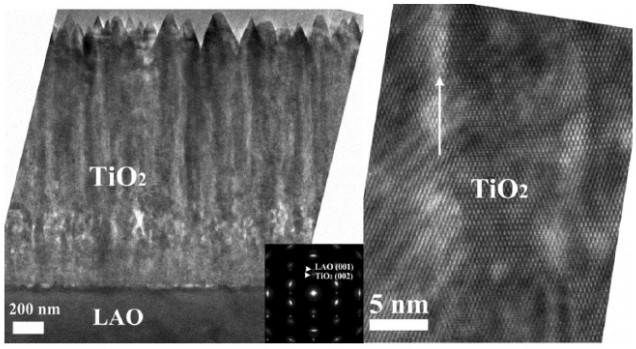

Figure 2: Cross-section TEM images of TiO_2 thin film deposited on (001) LAO substrate.

ing onto the former layer. This interesting structure can be explained by the lattice mismatch between the thin film and the substrate. Since the lattice mismatch between LAO (a = 3.791Å) and anatase TiO_2 (a = 3.7852Å) is only -0.2%, there should be a small strain in the interface. As the film grows thicker, the film will maintain its own crystal structure rather than distorting itself for epitaxial growth, which cause the formation of nanopillar to release the epitaxial strain. Figure 3 shows the SEM image of the TiO_2 thin film surface, which confirms ordered nanopillar alignment.

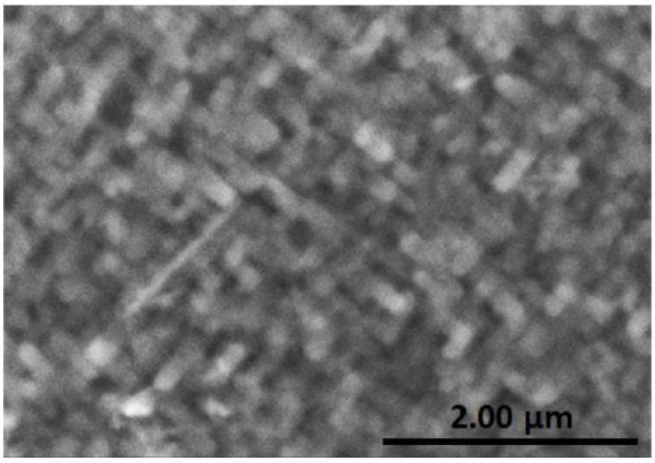

Figure 3: SEM image of anatase TiO_2 thin film on LAO substrate.

It was found that Ti^{4+} was stabilized below pH of 2.5 in the Ti-EDTA complex, and above pH, the Ti-EDTA complex tended to hydrolyze to colloidal TiO_2. Herein this experiment, by adding PEI into the precursor solution, no precipitates were detected in the solution with a wide range of pH from 1 to 10, which is a clear evidence that PEI served as binding regent to stabilize titanium complexes. Also, in the hydrothermal reaction, when the reactor was heated to 200°C, the pressure in autoclave increased significantly. Though the Ti-EDTA-PEI complex was very stable at ambient conditions, relative high temperatures and high pressures could accelerate the hydrolysis of titanium. Figure 4 shows the XRD patterns of TiO_2 thin film prepared in different reaction conditions. The thin film can be identified from the existence of anatase (004) peak in the XRD pattern. The hydrothermal reaction time varies from 6 to 24 h and the reaction temperature varies from 150 to 200°C. Thin film was not formed when the reaction time was less than 12 hours or reaction temperature was under 200°C. It can be seen that longer reaction time and higher reaction temperature increase the thickness of the TiO_2 thin film. Further

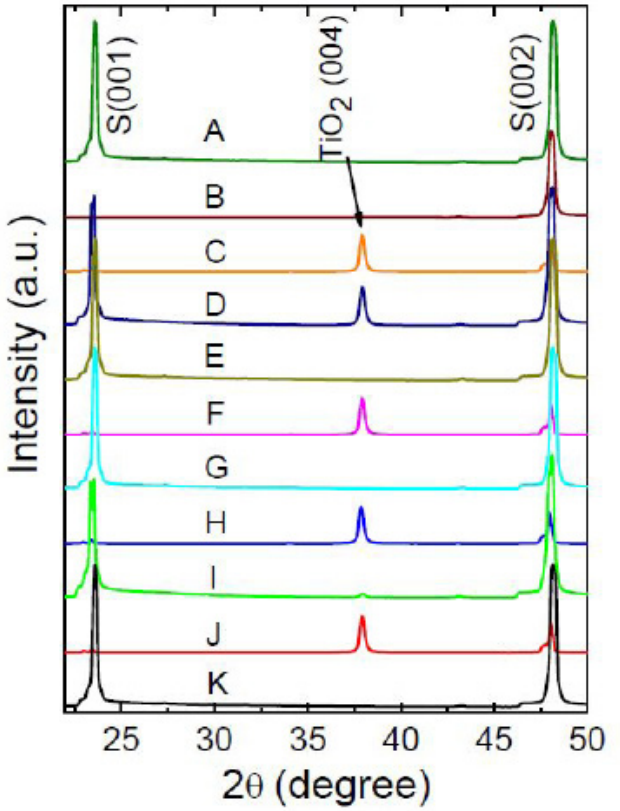

Figure 4: XRD patterns of TiO_2/LAO in different reaction conditions shown in Table 1.

increasing the growth time to 24h, the thickness of the thin film can reach 2.4µm, which is much thicker than epitaxial thin film prepared by traditional sol- gel spin-coating or dip-coating [22]. Compared with other reported hydrothermal to thin films [24-27], where the precursor solutions are not clear solution, this polymer-assisted hydrothermal method provides clear and table solution and has obvious advantages on obtaining films with varied thickness without repeating spin-coatings. Meanwhile, the influence of solution pH was also investigated. In acidic condition with pH at 4, no thin film was formed. It can be expected that strong acidic condition may induce severe and fast hydrolysis of titanium precursor, in which the nucleation of TiO_2 nanoparticles could be competitive to the thin film deposition. In neutral condition, the titanium precursor could mildly hydrolyze to deposit on the substrate. When the pH went up to 10, only part of the substrate was covered with TiO_2 thin film. The Ti-EDTA complex is very stable at this condition, which may weaken the attraction to PEI. As we expect, PEI could serve as template in the thin film formation, the hydrolysis process become unpredictable when the template effect is weaker. Besides, the precursor concentration effect was also investigated. When the concentration was 200 mM, no thin film was found on the substrate. The aforementioned nanoparticles nucleation may play an important role in the reaction process. At higher concentration, the hydrolyzed precursor can form more nuclei, which directly induced the formation of nanoparticles rather than thin film deposition.

SiO_2-embedded TiO_2 thin films were deposited on LAO substrates by using precursor solutions with different SiO_2 concentration to titanium concentration ratios. It is noted

that amorphous SiO_2 nanoparticles won't affect the epitaxial growth of TiO_2 on LAO substrates [28], therefore, the SiO_2 nanoparticles embedded in TiO_2 films are still epitaxial. The energy dispersive X-ray spectroscopy (EDS) was carried on SiO_2- embedded TiO_2 thin films to analyze its composition. With a sample prepared from precursor solution in which the concentration of SiO_2 is approximately half of that of Ti4+, the detected weight ratio of Si/Ti is 26.7%, corresponding to the atomic ratio of Si/Ti is 45.6%. The AFM images of pure and SiO_2-embedded TiO_2 thin film on LAO substrate are shown in Figure 5. As observed, the pure TiO_2 formed a uniform thin film on LAO substrate without any detectable microcracks, and the root-mean-square surface roughness is 16nm. With adding SiO_2, both of the grain size and roughness increase compared to those in pure TiO_2 thin films.

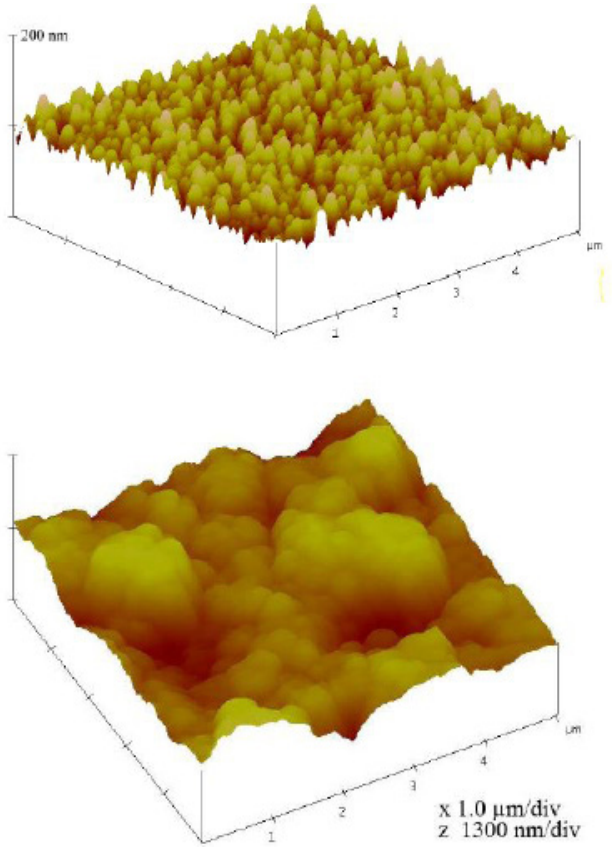

Figure 5: AFM images of TiO_2 thin film on LAO substrate. (a) without SiO_2 embedded; (b) with SiO_2 embedded.

TiO_2 directly grown on nickel foam was prepared by the same method for the anode of lithium ion batteries. This one-step synthesis method gives a convenient way to prepare anode materials. In addition, this binder-and-conductive carbon-free process made the contact between TiO_2 and current collector (nickel foam) more stable and improved the volumetric utilization efficiency [30]. Figure 6 shows the capacity as a function of cycle numbers at a current density of 100mA/g. It is observed that pure TiO_2 has a capacity of 144mAh/g after 30 cycles, and SiO_2-embedded TiO_2 has a much higher capacity 270 mAh/g. This can be understood by considering the reaction mechanism and the structure difference bringing by SiO_2 mixing. TiO_2 is one of the transitional metal oxides following Li insertion storage mechanism [38]. With embedded SiO_2, the crystalline structure of TiO_2 was destroyed to some degree,

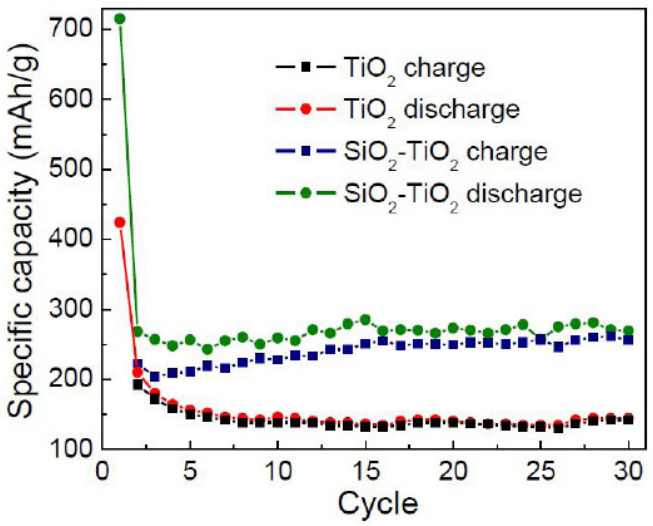

Figure 6: Cycle performance of pure and SiO_2-embedded TiO_2 at a current density of 100mA/g.

which induced a large amount of structure disorders and defects supplying more spaces for insertion of Li ions [31]. Therefore, the Li- diffusion of SiO_2-embedded TiO_2 is much higher than that of pure TiO_2. In addition, the specific capacity of SiO_2-embedded TiO_2 increases slightly as cycle number increases. The structure defects caused by embedded SiO_2 make the crystal lattice unstable and therefore much easier to be influenced by the lattices around. As the charge-discharge processes go on, more TiO_2 were activated and involved in reaction. The electrochemical performance of SiO_2-embedded TiO_2 is much better than that of other nanostructured TiO_2. Mesoporous TiO_2-C nanospheres deliver a capacity of ~170mAh/g at a current density of ~96mA/g [33]. Nanostructures TiO_2–graphene hybrid has a capacity of ~190mAh/g at a current density of 84mA/g and ~160 mAh/g at 168mA/g [37]. TiO_2 mesoporous nanocrystalline microspheres demonstrate capacities of 265, 234, 182, 175, and 156mAh/g at the discharge rates of 0.06, 0.12, 0.3, 0.6, and 1.2 C (1 C corresponds to 170mA/g) [34].

Conclusion

Pure and SiO_2-embedded epitaxial TiO_2 thin film on LAO substrates have been synthesized via a novel polymer-assisted hydrothermal approach. An interesting two- layer structure was found with well-aligned nanopillars to release the strain in epitaxial growth. The nanoparticles nucleation is shown to be a strong competitive process in the thin film growth, which could be suppressed by lowering the precursor concentration and adjusting the precursor solution to a neutral pH condition. With SiO_2 mixing, the grain size and roughness of the thin film increase. Moreover, this one-step hydrothermal synthesis process can be used to prepare anode materials for lithium ion batteries as well. This binder-and-conductive carbon-free process made the contact between anode material and current collector more stable and improved the volumetric utilization efficiency. Since EDTA and PEI can bind to most of the metal ions to produce stable complex, this polymer-assisted hydrothermal approach could be generalized to other metal oxide systems in epitaxial thin film synthesis and also in the preparation of polycrystalline anode materials for lithium ion batteries.

Acknowledgements

We acknowledge the support from NSF under Grant No. 1131290. The cross-sectional TEM images were taken by Prof. H. Wang in University of Texas A & M.

References

1) Reddy KM, Manorama SV, Reddy AR (2003) Bandgap studies on anatase titanium dioxide nanoparticles. Mater Chem Phys 78: 239-245.

2) Wang YQ, Hu GQ, Duan XF, Sun HL, Xue QK (2002) Microstructure and formation mechanism of titanium dioxide nanotubes, Chem Phys Lett 365: 427-431.

3) Yuan ZY, Su BL (2004) Titanium oxide nanotubes, nanofibers and nanowires. Colloids and Surf A: Physicochem and Engineer Aspects 241: 173-183.

4) Luo HM, Takata T, Lee Y, Zhao JF, Domen K, et al. (2004) Photocatalytic activity enhancing for titantium dioxide by co-dopingwith bromine and chlorine. Chem Mater 16: 846-849.

5) Mu Q, Li Y, Wang H, Zhang Q (2012) Self-organized TiO_2 nanorod arrays on glass substrate for self-cleaning antireflection coatings. J Colloid Interface Sci 365: 308-313.

6) Yu JC, Zhang, LZ, Zheng Z, Zhao JC (2003) Synthesis and characterization of phosphated mesoporous titanium dioxide with high photocatalytic activity. Chem Mater 15: 2280-2286.

7) Lee AC, Lin RH, Yang CY, Lin MH, Wang WY (2008) Preparations and characterization of novel photocatalysts with mesoporous titanium dioxide (TiO_2) via a sol-gel method. Mater Chem Phys 109: 275-280.

8) Caruso RA, Schattka JH, Greiner A (2001) Titanium dioxide tubes from sol–gel coating of electrospun polymer fibers. Adv Mater 13: 1577-1579.

9) Kawakita M, Kawakita J, Sakka Y (2010) Material properties controlling photocurrent on TiO_2 aggregates with plane orientation for dye-sensitized solar cells. J Nanopart Research 12: 2621-2628.

10) O'Regan B, Gratzel M (1991) A low-cost, high-efficiency solar cell based on dye- sensitized colloidal TiO_2 films. Nature 353: 737-740

11)Goh GKL, Chan KYS, Liu T (2011) Hydrothermal epitaxy of ferromagnetic cobalt doped titanium dioxide films at 120 degrees C. CrystEngComm 13: 524-529.

12) Lindgren T, Mwabora JM, Avendano E, Jonsson J, Hoel A, et al. (2003) Photoelectrochemical and optical properties of nitrogen doped titanium dioxide films prepared by reactive DC magnetron sputtering, J Phys Chem B 107: 5709-5716.

13) Lobl P, Huppertz M, Mergel D (1994) Nucleation and growth in TiO_2 films prepared by sputtering and evaporation. Thin Solid Films 251: 72-79.

14) Murugesan S, Kuppusami P, Parvathavarthini N, Mohandas E (2007) Pulsed laser deposition of anatase and rutile TiO_2 thin films. Surf Coatings Technol 201: 7713-7719.

15) Suda Y, Kawasaki H, Ueda T, Ohshima T (2004) Preparation of high quality nitrogen doped TiO_2 thin film as a photocatalyst using a pulsed laser deposition method, Thin Solid Films 453: 162-166.

16) Matsumoto Y, Murakami M, Hasegawa T, Fukumura T, Kawasaki M, et al. (2002) Structural control and combinatorial doping of titanium dioxide thin films by laser molecular beam epitaxy. Appl Surf Sci 189: 344-348.

17) Osterwalder J, Droubay T, Kaspar T, Williams J, Wang CM, et al. (2005) Growth of Cr-doped TiO_2 films in the rutile and anatase structures by oxygen plasma assisted molecular beam epitaxy. Thin Solid Films 484: 289-298.

18) Lotnyk A, Senz S, Hesse D (2007) Epitaxial growth of TiO_2 thin films on $SrTiO_3$, $LaAlO_3$ and yttria-stabilized zirconia substrates by electron beam evaporation. Thin Solid Films 515: 3439-3447.

19) Sandell A, Anderson MP, Alfredsson Y, Johansson MKJ, SchnadtJ, et al. (2002) Titanium dioxide thin-film growth on silicon (111) by chemical vapor deposition of titanium (IV) isopropoxide. J Appl Phys 92: 3381.

20) Nizard H, Kosinova ML, Fainer NI, Rumyantsev Yu M, Ayupov BM, et al. (2008) Deposition of titanium dioxide from TTIP by plasma enhanced and remote plasma enhanced chemical vapor deposition. Surf Coatings Technol 202: 4076-4085.

21) Jia QX, McCleskey TM, Burrell AK, Lin Y, Collis GE, et al. (2004) Polymer-assisted deposition of metal-oxide films. Nature Mater 3: 529-532.

22) Fei L, Naeemi M, Zou G, Luo HM (2013) Chemical solution deposition of epitaxial metal-oxide nanocomposite thin films. The Chem Record 13: 85-101.

23) Zou G, Zhao J, Luo HM, McCleskey TM, Burrell AK, et al. (2013) Polymer-assisted deposition: a chemical solution route for a wide range of materials growth. Chem Soc Rev 42: 439-449.

24) Hou RZ, Wu AY, Vilarinho PM (2009) Low-Temperature Hydrothermal Deposition of $(Ba_xSr_{1-x})TiO_3$ Thin Films on Flexible Polymeric Substrates for Embedded Applications. Chem Mater 21: 1214–122.

25) Chan KYS, Goh GKL (2009) Solution Epitaxy of TiO_2 Thin Films, J Electrochem Soc 156: D231-D235.

26) Wang X, Chen L, Zhao J, Jin L, Li L (2008) Hydrothermal synthesis of thin films of barium titanate nanotube arrays. Integrated Ferroelectrics 99: 125–131.

27) Sun K, Wei W, Ding Y, Jing Y, Wang Z, et al. (2011) Crystalline ZnO thin film by hydrothermal growth. Chem Commun 47: 7776–7778.

28) Luo HM, Lin Y, Wang H, Baily SA, Lee JH, et al. (2008) Amorphous silica nanoparticles embedded in epitaxial $SrTiO_3$ and $CoFe_2O_4$ matrices. Angew Chemie Int Ed 47: 5768-5771.

29) Jiang YF, Chen G, Xu X, Chen X, Deng S, et al. (2014) Direct growth of mesoporous anatase TiO_2 on nickel foam by soft template method as binder-free anode for lithium-ion batteries. RSC Adv 4: 48938-48942.

30) Ryu WH, Nam DH, Ko YS, Kim RH, Kwon HS (2012) Electrochemical performance of a smooth and highly ordered TiO_2 nanotube electrode for Li-ion batteries. Electrochimica Acta 61: 19– 24.

31) Fang H, Liu M, Wang D, Sun T, Guan D, et al. (2009) Comparison of the rate capability of nanostructured amorphous and anatase TiO_2 for lithium insertion using anodic TiO_2 nanotube arrays. Nanotechnol 20: 225701.

32) Armstrong G, Armstrong AR, Bruce PG, Reale P, Scrosati B (2006) TiO_2(B) nanowires as an improved anode material for lithium-ion batteries containing $LiFePO_4$ or $LiNi_{0.5}Mn_{1.5}O_4$ cathodes and a polymer electrolyte. Adv Mater 18: 2597–2600.

33) Cao FF, Wu XL, Xin S, Guo YG, Wan LJ (2010) Facile synthesis of mesoporous TiO_2-C nanosphere as an improved anode material for superior high rate 1.5 V rechargeable Li ion batteries containing $LiFePO_4$-C cathode. J Phys Chem C 114: 10308–10313.

34) Wang J, Zhou Y, Hu Y, O'Hayre R, Shao Z (2011) Facile synthesis of nanocrystalline TiO_2 mesoporous microspheres for lithium-ion batteries. J Phys Chem C 115: 2529-2536.

35) Guo YG, Hu YS, Sigle W, Maier J (2007) Superior electrode performance of nanostructured mesoporous TiO_2 (anatase) through efficient hierarchical mixed conducting networks. Adv Mater 19: 2087-2091.

36) Yang MC, Lee YY, Xu B, Powers K, Meng YS (2012) TiO_2 flakes as anode materials for Li-ion-batteries. J Power Sources 207: 166-172.

37) Wang D, Choi D, Li J, Yang Z, Nie Z, et al. (2009) Self-assembled TiO_2–graphene hybrid nanostructures for enhanced Li-ion insertion. ACS Nano 3: 907-914.

38) Ji L, Lin Z, Alcoutlabi M, Zhang X (2011) Recent developments in nanostructured anode materials for rechargeable lithium-ion batteries. Energy Environ Sci 4: 2682-2699.